A comparative study of MOND and MOG theories versus the κ-model: An application to galaxy clusters

Gianni Pascoli

Title A comparative study of MOND and MOG theories versus the κ-model: An application to galaxy clusters

G. Pascoli

Email: pascoli@u-picardie.fr

Faculté des sciences

Département de physique

Université de Picardie Jules Verne (UPJV)

33 Rue Saint Leu, Amiens, France

Abstract Many models have been proposed to minimize the dark matter (DM) content in various astronomical objects at every scale in the Universe. The most widely known model is MOdified Newtonian Dynamics (MOND). MOND was first published by Mordehai Milgrom in 1983 (Milgrom, 1983; 2015; see also Banik and Zhao, 2022 for a review). A second concurrent model is modified gravity (MOG), which is a covariant scalar-tensor-vector (STVG) extension of general relativity (Moffat, 2006; 2020). Other theories also exist but have not been broadly applied to a large list of astronomical objects (Mannheim and Kazanas, 1989; Capozziello and De Laurentis, 2012; O'Brien and Moss, 2015; Verlinde, 2017). Eventually, we can also mention the Newtonian Fractional-Dimension Gravity (NFDG) (Varieschi, 2020, 2023), a gravity theory based on spaces with fractional (i.e., non-integer) dimension (Varieschi, and Calcagni, 2022; Calcagni, 2012).

A new model, called κ-model, based on very elementary phenomenological considerations, has recently been proposed in the astrophysics field. This model shows that the presence of dark matter can be considerably minimized with regard to the dynamics of galaxies (Pascoli, 2022 a,b). The κ-model belongs to the general family of

theories descended from MOND. Under this family of theories, there is no need to develop a highly uncertain dark matter sector of physics to explain the observations.

Keywords: dark matter, MOND, modified gravity, κ-model, galaxies, galaxy clusters

1 Introduction

The dark matter (DM) paradigm is considered to simply explain the dynamics in individual galaxies and galaxy clusters. Astrophysicists have been searching for DM evidence for years. However, the quantity of dark matter required is immense, and the ratio of the dark matter (DM) to the baryonic component (B), (DM/B), could largely exceed 10 in a few galaxy clusters, raising serious doubts about the validity of this hypothesis. A rapid explanation to remedy this problem is to say that a large quantity of invisible baryonic matter is not counted in the galaxies and galaxy clusters. Unfortunately, this immediate solution is may be acceptable up to a factor of 2, but fully irrealistic up to a factor of 10. What is then the nature of dark matter ? To date, no particle of dark matter has never been detected in lab (DAMA/LIBRA Collaboration, 2022), even though researchers have built larger and more sensitive detectors (Xenon Collaboration, 2023). This is rather an intriguing status and the DM paradigm sounds suspiciously similar to the phlogistic and the aether in the nineteenth century. Additionally, some agnostic physicists believe that DM does not exist at all and have instead proposed alternative models of gravity. As a result, all sorts of theories have been built in order to remove dark matter in all astrophysical systems. There are two theories that stand out because they have been applied to

numerous concrete situations. The first is modified Newtonian dynamics (MOND). MOND diverges from the standard Newton's laws at extremely low accelerations, which are a characteristic of the outer regions of galaxies (Milgrom, 1983, 2015). MOND postulates a modification to Newton's second law, such that the force applied on a particle is no longer proportional to the acceleration a, but rather to its square a^2, when the accelerations are smaller than the critical limit $a_0 = 10^{-10}\ ms^{-2}$ (Milgrom, 1983). This model effectively explains the dynamics of individual galaxies without dark matter (Famey and Mc Gaugh, 2012).

In modified gravity (MOG) (STVG or scalar-tensor-vector gravity), the approach is very different. The structure of space-time is described by the usual metric tensor $g_{\mu\nu}$, complemented by a vector field, ϕ_μ, and two scalar fields, G and μ, which represent a dynamical version of the Newtonian gravitational constant and the mass of the vector field, respectively (Moffat, 2006; 2020). The vector field part produces a Yukawa-like modification of the gravitational force due to a point source. This model accurately explains not only the dynamics of galaxies but also the dynamics in galaxy clusters without dark matter (Moffat, 2020).

The common and main objective of MOND and MOG theories is to eliminate in whole or in part the dark matter in the Universe. The agreement between these two models and the observational data are very remarkable for galactic dynamics; however, the situation is distinct for galaxy clusters where MOG appears to have an advantage over its competitor MOND (Brownstein and Moffat, 2006). MOG achieves to eliminate all dark matter content in these objects, but MOND still needs to consider some form of invisible matter in galaxy clusters (Mc Gaugh, 2015). However, this does not mean that MOND has been falsified, because the MONDian world is very rich

and there are numerous extensions, such as the promising extended MOND (EMOND) (Hodson and Zhao, 2017a, b)[1]. Moreover, we can speculate whether MOG does not reintroduce DM in a disguised manner (the vector field ϕ_μ is massive). Following this simple statement, only MOND is truly free of DM, and the path followed by EMOND is potentially preferable.

The third model studied here is the κ-model; it is based on a phenomenological and MONDian procedure whose main aim is to simultaneously explain the dynamics of individual galaxies by minimizing the dark matter content and by maintaining the formal aspect of the Newtonian law of gravitation. It is based on a relational consideration; the mean density of matter is estimated at a very large scale, and the surroundings of a given observer influence the measurements made for the determination of the velocities and accelerations. In this regard, the observations depend not only on the reference frame of the observer but also on his environment. Thus, the κ-model uses a holistic or Machian approach. The velocities and accelerations that are environment-dependent are renormalized, and the observer measures apparent quantities depending on a coefficient denoted κ. An empirical (and universal) relationship is provided between the coefficient κ and the mean density. The coefficient κ intervenes in the acceleration term of the dynamics equation and imparts a MOND-type appearance to the κ-model. However, a physical support is now provided; this is the environment of the observer, which distorts the measurements. Thus, a naive analogy is that of an observer placed in a medium of given refraction index, who sees a magnification of both the size and the velocity of any object. However, this very simplistic comparison is not to be taken at face value because in a

[1]The most complete theory regarding the MONDian world is that of Solznik and Skordis (2021), but the formalism EMOND is much easier to manipulate (the theory of Solznik and Skordis belongs to the large class of TeVeS theories, such as MOG with many free parameters and some disguised aspect of DM).

medium of given refraction index, the light is attenuated and the images can be extremely blurred. On the contrary, in the κ-model framework, no such medium is existing; the light is not attenuated and it still propagates in straight line with the speed c, constant and independent of frequency, as measured in vacuum by every observer (Pascoli, 2022a)[2]. The great interest of the κ-model is that no arbitrary parameter is introduced, contrary to MOG, which has two outer free parameters (these two models having a universal relationship for the fits). Another advantage of the κ-model is that it would permit to pass directly for any type of galaxies from the data on the spectroscopic velocity measurements to the mean densities (and inversely) without the ambiguous transition through the mass-to-light ratio knowledge. The relationship between the spectroscopic velocities and the mean densities is direct in the κ-model. Strongly contrasting with this view, DM can fit almost all rotational curves with any mean baryonic density profiles due to its very large flexibility, and for this reason the DM paradigm has unfortunately no predictive value. Eventually the κ-model can easily help to understand the weaker "DM effect" in the regions where the mean density is high (globular clusters, core of the galaxies) and, conversely, the stronger "DM effect" in the regions where the mean density is weaker (outer regions of the galaxies, low brightness galaxies and galaxy clusters). More specifically, the κ-model predicts that when the mean density $\bar{\rho}$ in a large-scale object (galaxy or galaxy cluster) is smaller than

[2]Further information is summarized in the two appendices A and B placed at the end of this paper. Initially, we start with an isotropic and homogeneous base space Σ. In this space the light propagates in straight line. However, any observer is located at the center of a homogeneous and isotropic universe $\kappa\Sigma$, homothetic to the base space Σ; the coefficient κ is dependent on the environment of this observer (the mean density of matter surrounding the observer). Unfortunately, it is very difficult to have a global view of the situation with a unique $\mathbb{R}^3$-type space. Rather, the image needs to be that of a fiber bundle $\Sigma \times \kappa$ with Σ as the base and κ as the fiber (specifically, each observer projects all structures present in the Universe on his own stratum labelled by κ). Within the framework of this fiber bundle, DM effects can be re-interpreted as a κ-lensing, whose the Bullet Cluster is an illustrative example (paragraph 3).

a critical value $\sim$ 4 10^{-24} $g\ cm^{-3}$[3] the measured velocities appear magnified compared to the estimated newtonian velocities.

The κ-model has been already applied to various types of galaxies, such as large or small low surface brightness galaxies (LSBs) and high surface brightness galaxies (HSBs) (Pascoli, 2022 a,b). The κ-model fits and the observational curves has been shown in fairly good agreement. Even though this study needs to be extended to a larger database, such as SPARC (Lelli, McGaugh and Schombert; 2017), these initial results and deductions provided by the κ-model are highly encouraging.

While the κ-model appears to succeed at explaining the dynamics of numerous individual galaxies (Pascoli, 2022), to date, this model has not been tested on the galaxy cluster field, and this is the goal of our present study. We show that the κ-model can greatly lower the major part of the dark matter content in the galaxy clusters. The current ratio DM/B amounts around 10 in the outskirts of these objects, and the κ-model can reduce this ratio to approximately $0 - 1$. The situation is more difficult in the inner regions of the galaxy clusters, but by lowering the gas temperature in these regions, the problem can be easily solved. The κ-model provides a good predication for the ratio DM/B in the outer regions of galaxy clusters, without introduction of numerous free parameters other than those linked to the mean density of baryonic matter (Pascoli, 2022 a,b). Likely, this result is not a mere coincidence, and supports the consideration of our new proposal. Here, the κ-model is applied to a sample of galaxy clusters (paragraph 2) and then, eventually, to the Bullet Cluster (paragraph 3).

[3]This value corresponds to the mean density of the baryonic matter detected in the solar neighborhood (or, correspondingly, $\sim 70\ M_\odot\ pc^{-2}$, assuming a vertical thickness $\sim 1\ kpc$ (Famaey, and McGaugh, Fig.19, 2012)).

2 Quick review of the κ-model

In this section we summarize the main ideas developed in the preceding papers (Pascoli and Pernas, 2020; Pascoli, 2022 a, b) as for the motion of an individual particle seen in a frame of reference. The appendix A specifies what we mean by frame of reference in the approach of the κ-model.

In a current manner for a terrestrial observer E the motion of any particle of mass m is simply determined by the following dynamic equation:

$$m\frac{d(\kappa_E\dot{\boldsymbol{\sigma}})}{dt} = \boldsymbol{f}_E \tag{1}$$

where $\dot{\boldsymbol{\sigma}}$ is the bare velocity of the particle (the point on $\boldsymbol{\sigma}$ designates the derivative of the bare position of the particle given by $\boldsymbol{\sigma}$) and $\boldsymbol{f}_E$ is the sum of forces applied to it[4], as evaluated by the observer E (the coefficient κ is defined below). Additionally, the κ-model assumes that at a very large (galactic) scale, the immediate environment of a particle plays a role in the determination of its motion. For instance, the particle "feels" the presence of the other particles in such a way that its velocity is modified by a scale factor κ that is proportional to the mean density $\bar{\rho}$; more exactly, this factor is proportional to the logarithm of the mean density. In a more concrete manner, all structures of the Universe are usually inserted in a homogeneous and isotropic base space Σ with coordinates $\boldsymbol{\sigma}$. A phase space $\Pi(\boldsymbol{\sigma}, \dot{\boldsymbol{\sigma}})$ is attached to Σ (the point on the letter designates the time derivative). However, every observer O has his own measuring gauge, which is dependent on his environment. Thus, this observer applies an apparent isotropic and homogeneous dilation to

[4]The force $\boldsymbol{f}$ is the resultant force of the gravitational, electrostatic and magnetic forces, and also of the centrifugal and Coriolis forces if the frame of reference is not inertial.

the phase space $\Pi(\boldsymbol{\sigma}, \dot{\boldsymbol{\sigma}})$[5]

$$(\boldsymbol{\sigma}, \dot{\boldsymbol{\sigma}}) \longrightarrow (\kappa\boldsymbol{\sigma}, \kappa\dot{\boldsymbol{\sigma}}) \tag{2}$$

where κ is a renormalization coefficient (for the terrestrial observer κ is denoted κ_E). For any observer O, the coefficient κ is considered to be independent of the point, and any other observer O', placed in a distinct environment, follows the same reasoning, but with the essential difference that this one applies a coefficient $\kappa' \neq \kappa$. The basic idea is that any observer does not directly access to the phase space Π but rather visualizes an apparent homothetic replica $\kappa\Pi$. The κ-model is reduced to this sole operation. Consequently, this model is not a "theory" by itself. An underlying theory is needed, such as the Newtonian mechanics or the general relativity.

For any extended objects (a galaxy or a galaxy cluster) with a mean density profile with both definite upper ρ_M and lower ρ_m bounds, such as $\rho_M > \rho_m$, there exists a universal relationship for κ; this factor is linked to the local mean density $\bar{\rho}$, as follows:

$$\frac{\kappa_M}{\kappa} = 1 + Ln(\frac{\rho_M - \rho_m}{\bar{\rho} - \rho_m}) \tag{3}$$

For a galaxy or a cluster of galaxies $\rho_M \gg \rho_m \simeq 0$, this relationship simplifies in the form $\frac{\kappa_M}{\kappa} = 1 + Ln\,(\frac{\rho_M}{\bar{\rho}})$ (the function $\bar{\rho}$ has a definite upper bound ρ_M and $\rho_m \simeq 0$)[6]. The quantity ρ_M is a reference value for the mean density. For any local observer the density measured,

[5]Once this operation is achieved, the quantity $\kappa\boldsymbol{\sigma}$ forms an inseparable unit $\boldsymbol{R}$, where κ and $\boldsymbol{\sigma}$ are no longer separately measurable for any observer (similarly for $\kappa\dot{\boldsymbol{\sigma}}$, which forms an inseparable unit $\dot{\boldsymbol{R}}$). Within the κ-model framework the Newtonian law is formally maintained, as follows: $m\frac{d\boldsymbol{P}}{dt} = -\boldsymbol{\nabla}_{\boldsymbol{R}}[(\Phi(\boldsymbol{R})]$ where $\boldsymbol{P} = m\dot{\boldsymbol{R}}$ is the impulsion of the particle and Φ is the gravitational potential measured in situ. For all these reasons the variation of κ is hidden to any observer, and the space Σ of vectors $\boldsymbol{\sigma}$ is not reachable. However, the ratios of the type $\frac{\kappa'}{\kappa}$ are always measurable for any observer, an operation which helps to exchange the information with other observers (Pascoli, 2022).

[6]However, in order to perform the analysis of the CMB in the framework of the $\kappa-$model, the complete form has to be used because $\rho_M \simeq \rho_m$ ($\frac{\rho_M - \rho_m}{\rho_m} \sim 10^{-5}$).

$\bar{\rho}_l$, is equal to the following:

$$\frac{\bar{\rho}}{\left[1 + Ln\left(\frac{\rho_M}{\bar{\rho}}\right)\right]^3} \tag{4}$$

The density $\bar{\rho}_l$, measured in situ, can be considered as real, whereas the density $\bar{\rho}$ measured by a terrestrial observer is only an "apparent" quantity. Eventually, the mean density around a point, labelled by $\boldsymbol{\sigma}$, can be obtained by integrating over a suitably sized volume ω surrounding this point as follows:

$$\bar{\rho}(\boldsymbol{\sigma}) = \int_{\omega} d^3\boldsymbol{\sigma}' w(\boldsymbol{\sigma} - \boldsymbol{\sigma}')\rho(\boldsymbol{\sigma}') \tag{5}$$

For simplicity, we can assume that the spread function $w(\boldsymbol{\sigma})$ is isotropic and Gaussian, i.e. $w(\boldsymbol{\sigma}) = (\pi\delta^2)^{(-3/2)} e^{-\left(\frac{\boldsymbol{\sigma}^2}{\delta^2}\right)}$. This spatial averaging is used to smooth the strongly varying density distribution of matter in a galaxy over distances of a few parsecs around each point.

By using the transform (2), the dynamic equation (1) can now be rewritten as follows:[7]

$$m\frac{d}{dt}(\kappa\dot{\boldsymbol{\sigma}}) = \left(\frac{\kappa_E}{\kappa}\right)^2 \boldsymbol{f}_E = \boldsymbol{f} \tag{7}$$

[7]The equation (1) is evidently not correct, and the well known consequence of its misuse constitutes the missing mass problem. The solution acknowledged today by a common consensus is to add dark matter. Thus, we have the following relationship:

$$m\frac{d}{dt}(\kappa_E\dot{\boldsymbol{\sigma}}) = \boldsymbol{f}_E + \boldsymbol{f}_{DM} = (1+\alpha)\boldsymbol{f}_E \tag{6}$$

The observations provides $\alpha \sim 1 - 10$, following the type of extended objects under consideration (the coefficient α, or more generally the profile of the function α when α varies in the objects, is predominantly adapted in an ad hoc manner). For instance, α is small in dense systems, such as globular clusters and, at the opposite side, high in diffuse low-density galaxies.

where the second equality is consistent with the following relationship:

$$\boldsymbol{f}_{C\longrightarrow P}=-GMm\frac{\kappa\mathbf{CP}}{\kappa^3 CP^3}=\left(\frac{\kappa_E}{\kappa}\right)^2\boldsymbol{f}_{E,C\longrightarrow P} \tag{8}$$

This relationship applies for a test particle P of mass m under the action of a central attractor C of mass M ($\boldsymbol{\sigma}=\boldsymbol{CP}$). The real force is evaluated where the particle P resides (the real force is measured in situ, contrarily to the force estimated by the terrstrial observer which is apparent).

For a particle placed on a circular orbit and subjected to a central attractor of mass M, the coefficient κ is quasi-constant, and the following relationship is obtained for the spectroscopic velocities:

$$\boldsymbol{v}^2_{spectro}=(\kappa\dot{\sigma})^2=\frac{\kappa_E}{\kappa}(\frac{GM}{\kappa_E\sigma}) \tag{9}$$

Introducing the apparent radial coordinate $r=\kappa_E\sigma$, we find

$$\boldsymbol{v}^2_{spectro}=(\frac{\kappa_E}{\kappa})(\frac{GM}{r}) \tag{10}$$

Two very distinct interpretations of the magnification factor $\frac{\kappa_E}{\kappa}$ are then possible: an apparent magnification of the gravitational constant G (as in MOG) or an apparent magnification of the attractive mass M (as in DM with the identification $1+\alpha=\frac{\kappa_E}{\kappa}$). Note that $\boldsymbol{v}^2_{spectro}$ is a real quantity, i.e. observer-independent (we can replace κ_E with any value); in other words any observer measures the same spectroscopic velocity as that valuated by an inertial observer, placed in situ (i.e. a local observer located where the emiter of the radiation resides).

We can choose the simple example of an archetypical spiral galaxy where the density is seen to vary following an exponential law as a function of r in the disk. Then by using the relation (3), we find that

the ratio $\frac{\kappa_E}{\kappa}$ varies as r. In this case the relation (9) naturally leads to a constant value for the spectroscopic velocity in the outskirts of this galaxy (Pascoli, 2022). In the κ-model the exponential profile for the density in the disk naturally implies the flatness of the rotation curves of the spiral galaxies. On the contrary in the DM model as the surface density of baryon matter declines in the outer regions of the disk, that of the dark matter must increase in an adhoc manner to reproduce the flatness.

Let us eventually notice that the renormalization of lengths (eq. 2), hypothesized in the κ-model, has very likely a link, with the MOND paradigm, where the modification of the inertia term is a kind of renormalization of the acceleration. For instance Zhao and Famaey (2012) have suggested that a rescaling of the MOND acceleration constant $a0$ would account for the exact spatial distribution of the residual missing mass in MOND clusters.

A link seems to be also existing between the κ-model and the Newtonian Fractional-Dimension Gravity (NFDG) (Varieschi, 2020). NFDG belongs to the large family of models of gravitational and matter (Calcagni, 2012). Especially NFDG is based on a variable dimension function considered as a field $D(r)$ depending on the radial coordinate r. This leads to a gravitational potential of the form $\sim \frac{1}{r^{(D-2)}}$, i.e. $\rightarrow \frac{1}{r}$, for $D \rightarrow 3$ (central bulky region of a galaxy) and $\rightarrow Lnr$ for $D \rightarrow 2$ (disk), yielding a flat galactic rotation curves in the outer regions of spiral galaxies. NFDG is equipped with an appropriate scale length l_0, and then the radial coordinate r is considered to be a rescaled dimensionless coordinate, i.e. $r\frac{1}{l_0}$. The scale length l_0 in NFDG is related to a_0 in MOND by $a_0 \approx GM/l_0^2$ for a galaxy of mass M.

Thus following all these MOND-like scenarios the missing mass

problem could eventually be solved by scale transforms depending on the size of the objects under consideration (the central region or the outskirts of a galaxy, a galaxy cluster, etc). This strong proposal is fundamentally different from the DM paradigm which assumes that 85% of the matter composing the Universe belongs to a dark sector of the physics which is totally unknown to us.

3 Galaxy clusters

The gas density profile for a galactic cluster can be approximately fitted by the following function (Cavaliere, and Fusco-Femiano, 1976):

$$\rho\left(r\right)=\rho_{M}\left[1+\left(\frac{r}{r_{c}}\right)^{2}\right]^{-\frac{3\beta}{2}} \tag{11}$$

where $\rho\left(r\right)$ is the intracluster medium (ICM) mass density profile and ρ_{M} is the maximal value taken by $\rho\left(r\right)$. r_{c} and β are fit parameters for the distribution of the density.

Due to this isotropic density distribution, the gas mass contained in a sphere of radius r is as follows:

$$M_{gas}(r)=4\pi\int_{0}^{r}drr'^{2}\rho\left(r'\right)={}_{2}F_{1}(1.5,\ 1.5\beta,2.5,-0.000017\ r^{2}) \tag{12}$$

where ${}_{2}F_{1}$ is the hypergeometric function.

When $r\gg r_{c}$ and $\beta<1$, we can approximate this formula by the more manipulable relationship, as follows:

$$M_{gas}(r)=\frac{4\pi\rho_{M}r_{c}^{3}}{3(1-\beta)}(\frac{r}{r_{c}})^{3(1-\beta)} \tag{13}$$

Unfortunately this relationship is clearly divergent when $r \longrightarrow \infty$. A cut-off for the distribution of gas, necessary for finite spatial extent, needs to be introduced. Following Brownstein and Moffat (2006), this cut-off, let rout, is chosen equal to the radius at which the density, drops to $10^{-28}\ g\ cm^{-3}$ or 250 times the mean cosmological density of the baryons.
On the other hand, assuming that the cluster is in hydrostatic (isothermal) equilibrium, the Newtonian dynamical mass is as follows (Brownstein and Moffat, 2006, eq. 19):

$$M_N\left(r\right) = \frac{3\beta\ k_B T}{\mu m_p G}\left(\frac{r^3}{r^2 + r_c^2}\right) \tag{14}$$

where T is the temperature, k_B is Boltzmann's constant, $\mu \approx 0.609$ is the mean atomic weight and m_p is the proton mass.

In eq.4 the quantities β, k_B, T, μ, m_p and G are κ-invariant, both r and r_c^{28} are transformed as $r \longrightarrow \frac{\kappa}{\kappa_E} r$. Then the κ-mass profile for a cluster is given by the following relationship:

$$M_\kappa(r) = \frac{\kappa}{\kappa_E} M_N(r) \tag{15}$$

where $M_N(r)$ is the Newtonian mass evaluated at the radius r. Then the mean density $\rho\left(r\right)$ is inserted in the relationship (κ, ρ) (see the appendix A eq. 18 placed at the end of the article) and this leads to the magnification ratio, as follows:

[8]The temperature T is measured in situ and is observer-independent, likewise for the dispersion velocities $\sigma_r, \sigma_\theta, \sigma_\phi$ (for instance in eq. 9 of Brownstein and Moffat, 2006 : $\sigma_r^2 = (k_B T)/\mu m_p$ is observer-independent, as is the gravitational potential Φ which is also measured in situ).

$$\frac{\kappa_E}{\kappa} = 1 + Ln\ \left(\frac{\rho_E}{\rho}\right) = 1 + Ln\left(\frac{\rho_E}{\rho_M}\frac{\rho_M}{\rho}\right)$$
$$= 1 + Ln\ \left(\frac{\rho_E}{\rho_M}\right) + \frac{3\beta}{2} Ln\left[1 + \left(\frac{r}{r_c}\right)^2\right] \quad (16)$$

with the mean mass density ρ_E near the Sun estimated to $4\,10^{-24}\ g\ cm^{-3}$. We used the sample of galaxy clusters from the paper of Brownstein and Moffat (2006). The relevant properties are listed in Table 1. By convention column (6) is the position, r_{out}, at which the density drops to $\rho_{out} \simeq 10^{-28}\ g\ cm^{-3}$, or 250 times the mean cosmological density of the baryons.

Figure 1 shows the results of our analysis applied to the COMA cluster. The κ-curve (shown in amber) has approximately the same profile as MOND (shown in dashed-dotted cyan) when $r > 100\ kpc$, but the κ-curve is much closer to the observational curve and even merges with the latter one in the outer regions of the cluster. Even though the κ-curve is not fully merged with the ICM gas curve inside the inner regions; however, the apparent gravitational mass has been largely lowered (by a factor in the range $7 - 10$ along the curve). Finally a residual gap has to be filled in between the κ-curve and the observational one in the inner regions of the COMA cluster. To do this, we propose to decrease the temperature in the inner regions. This proposal can be applied in the same way to the other galaxy clusters (Figure 2). Notably, in most of the cases presented on this array of figures, MOG theory leads exactly to the same prediction as the temperature profiles after comparing the curves (we can refer to A0085, A0133, NGC 507 and A062 as examples). Assuming a non-isothermal temperature profile, the Newtonian mass has to be re-calculated as follows (Brownstein and Moffat, 2006, eq. 18):

$$M_N\left(r\right) = \frac{r\ k_B T(r)}{\mu m_p G}\left(\frac{3\beta r^2}{r^2+r_c^2} - \frac{dLnT(r)}{dLn(r)}\right) \tag{17}$$

Then we used the following easy-to-manipulate temperature profile:

$$T\left(r\right) = T_{out} exp[-\alpha(\frac{r_{out}-r}{r_{out}})] \tag{18}$$

where T_{out} designates the temperature in the outer regions of the cluster. This parameter is provided in column (2) of Table 1. The coefficient $\alpha = 1$ is used when $M_N \lesssim 10\ M_{gas}$. This is the case for most situations under study. For a few cases where this ratio is far beyond 10, then $\alpha = 2$ is used. The temperature profile (eq.8) has been selected such that the outer temperature, T_{out} (column (7) of Table 1) is that provided by Brownstein and Moffat (2006), as directly resulting from observations (Reiprich and Böhringer, H. 2002).

$$M_N\left(r\right) = \frac{r\ k_B T(r)}{\mu m_p G}\left[\frac{3\beta r^2}{r^2+r_c^2} - \frac{\alpha r}{r_{out}}\right] \tag{19}$$

The green curve on the Figure 1 is the κ-profile with a non-isothermal temperature profile given by eq. 8. The κ-curve associated to a non-isothermal temperature profile becomes virtually superimposed to the ICM gas profile when $r < 500\ kpc$ (let us note that for $r > 500\ kpc$, the κ-curve, associated to an isothermal temperature profile and that associated to a non-isothermal temperature profile flank the ICM gas profile). Thus, a prediction of the κ-model is that the temperature is lowered by a factor two (at $r_{out}/2$) in the inner regions compared to that in the outskirts of the COMA cluster. More precisely, the most appropriate description is that of a non-isothermal core for $r < 1000\ kpc$, which is itself surrounded by a quasi-isothermal shell when $1000 < r < 1954\ kpc$. A vey simi-

lar situation is encountered in the other clusters collected in Table 1. Thus, since the κ-model has no outer parameters, an optimal fit can be achieved by finely adjusting the temperature profile and, in return, can eventually predict this profile (whereas this refinement and prediction are not possible within the ad hoc, and definitely not falsifiable, DM paradigm, which is easily adapted to fit the ICM gas curve with any temperature profile indicating no predictive value).

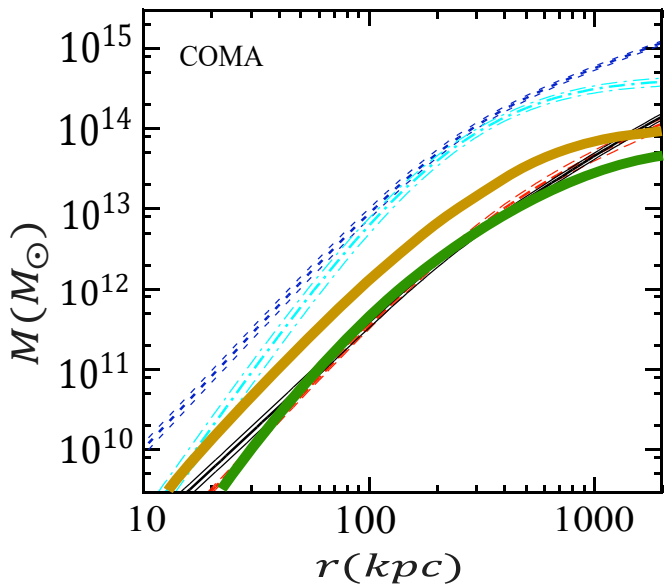

Figure 1 COMA cluster profile. The horizontal axis is the radius in kpc and the vertical axis is mass in units of the solar mass $M_\odot$. The red long dashed curve is the ICM gas mass derived from X-ray observations (compilation of Reiprich, 2001; Reiprich and Böhringer, 2002); the short dashed blue curve is the Newtonian dynamic mass; the dashed-dotted cyan curve is the MOND dynamic mass; the solid black curve is the MSTG dynamic mass (Browstein and Moffat, 2006). Our contribution is displayed as the amber curve, showing the κ-model dynamic mass with the temperature $T = 8.38\ keV$. The solid green curve displays the κ-model dynamic mass, assuming a non-isothermal temperature profile with $\alpha = 1$ in eq. 8.

A perfect superposition with the ICM gas mass curve in COMA cluster can still be achieved by taking the temperature profile displayed in Figure 2. We note an increase of the mean temperature from the inner regions up to 1500 kpc and then a slow decrease toward the outskirts. However, a comparison of this profile with observational data is not very conclusive. The main reason is that the COMA cluster modeled here, similar to other research (Browstein and Moffat, 2006), is in the form of a spherical and well-relaxed distribution of gas. The reality is much more complex. The density in the inner regions is relatively high, and the cooling through thermal bremsstrahlung emission must effectively be much more efficient than in the outskirts. However, the heating by active galactic nuclei in the inner regions can compensate for the cooling processes. Thus, the energetics are very complex and the temperature profile is not easily predicted (Bykov et al, 2015). In a general manner for the galaxy clusters, all temperature profiles found in the literature are model-dependent with a very large amount of dark matter. Moreover, even limiting to the outskirts, which are directly accessible, the physics is poorly understood (Walker et al, 2019). Thus, the temperature map of the outskirts of the COMA cluster simultaneously exhibits cool and hot regions with various substructures (Watanabe et al, 1999).

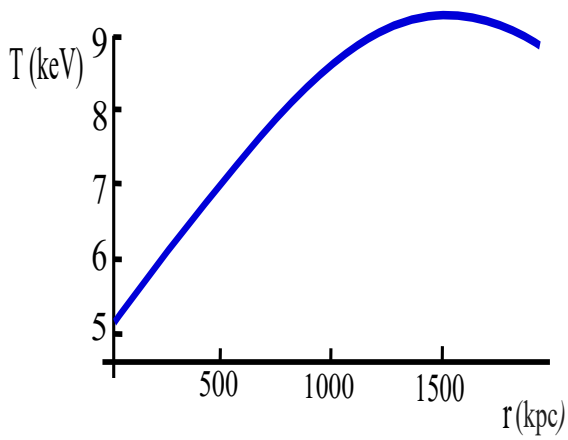

Figure 2 Predicted mean temperature profile in the COMA cluster

in the framework of the κ-model

We have suggested here to solve the problem of the very large excess of (newtonian) mass in the galaxy clusters by using a two-stage procedure. First, by significantly reducing the apparent attractive mass with the κ-model. With help of this operation the ratio M_{DM}/M_{gas} is reduced to rather more credible values, i.e. ~ 0 in the outer regions and to ~ 2 in the inner regions. Then the second step consists in adapting the temperature profile with cancellation of the residual excess of mass. It seems that MOG was facing the same situation, even though Brownstein and Moffat (2006) have not tried to perform this second step (for instance for A0085, ...). Another issue for this secong step would still be to follow the MOND galaxy cluster analysis of Banik and Zhao (2022), that is to say to add a dense core composed of sterile neutrinos (see Giunti and Lasserre (2019) for a review on these hypothetical particles). The observational data not being perfect it is very likely that a two-stage solution is also needed in the framework of other theories (for instance MOND) which have been proposed to eliminate the dark mater (taken into account of the measurement uncertainties of inclination, thickness, mass-to-light ratio for the individual spiral galaxies; density/temperature profiles and clumpiness in the case of galaxy clusters, and so on). The only model which runs directly in one step is dark matter given its undue flexibility (compared to the κ-model with no flexibility).

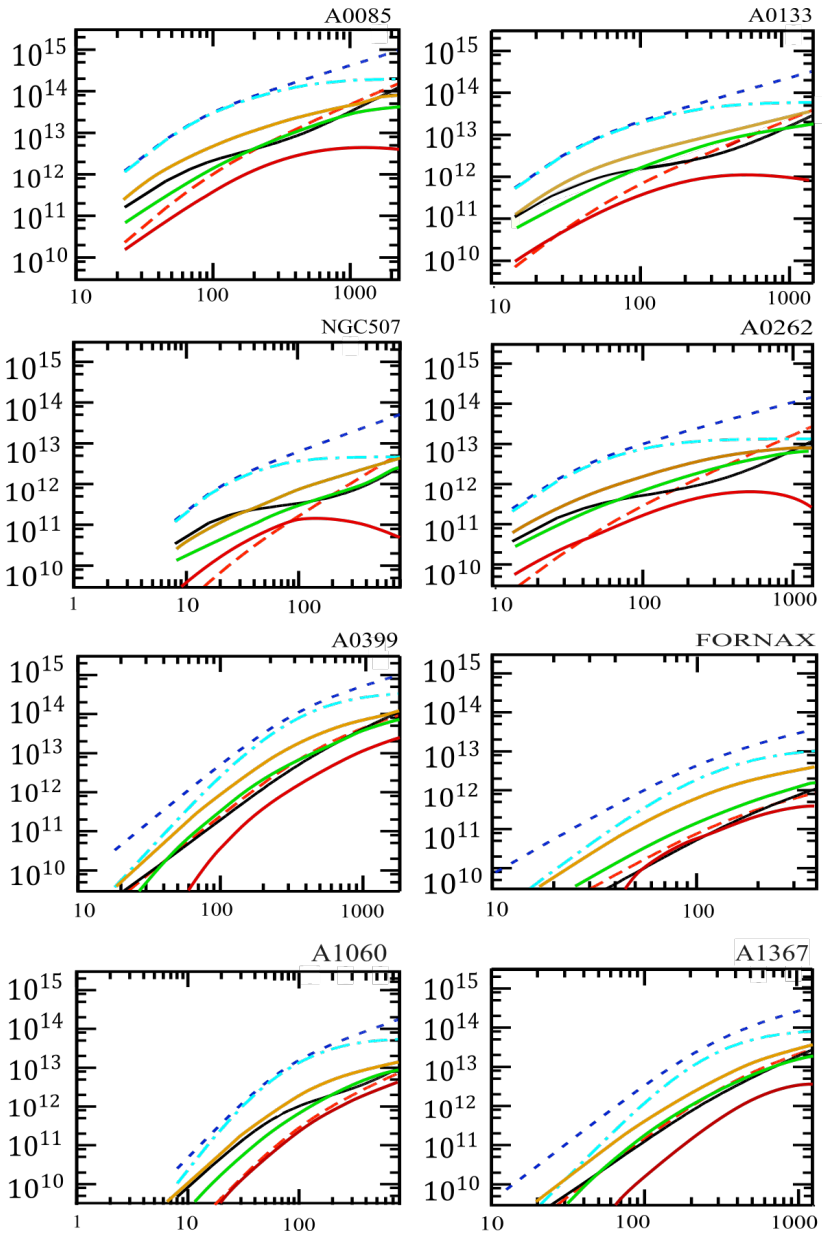

Figure 3 Plot of the radial mass profile for clusters of the sample in Table 1. The horizontal axis expresses the radius in *kpc* and the vertical axis is mass in units of solar mass $M_{\odot}$. The red long dashed curve is the ICM gas mass derived from X-ray observations (compilation of Reiprich, 2001; Reiprich and Böhringer, 2002); the short dashed blue curve is the Newtonian dynamic mass; the dashed-dotted cyan curve is the MOND dynamic mass; the solid black curve is the MSTG dynamic mass (Browstein and Moffat, 2006). Our contribu-

tion is displayed as the amber curve, showing the κ-model dynamic mass with the temperature $T = 8.38\ keV$. The solid green curve displays the κ-model dynamic mass, assuming a non-isothermal temperature profile with $\alpha = 1$ in eq. 8. The solid red curve displays the κ-model dynamic mass, with a non-isothermal temperature profile of $\alpha = 2$.

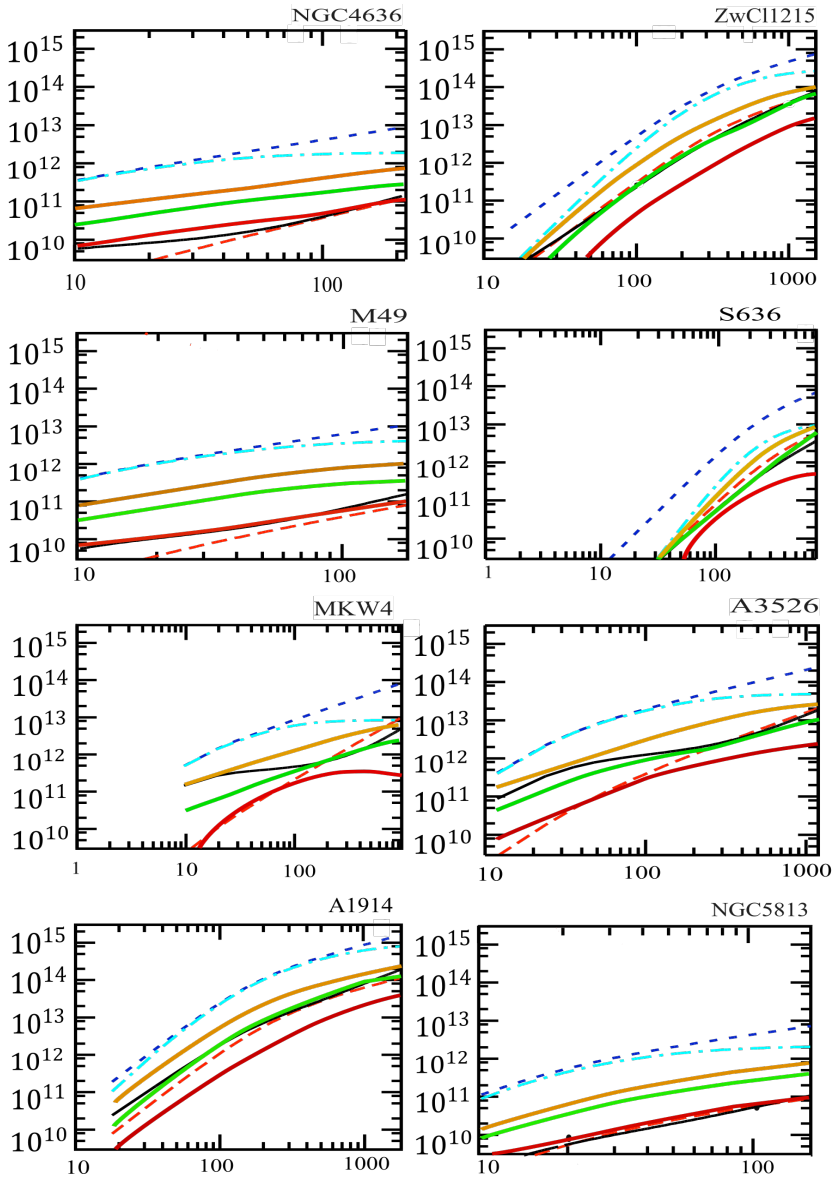

Figure 3 Continued galaxy cluster mass profiles

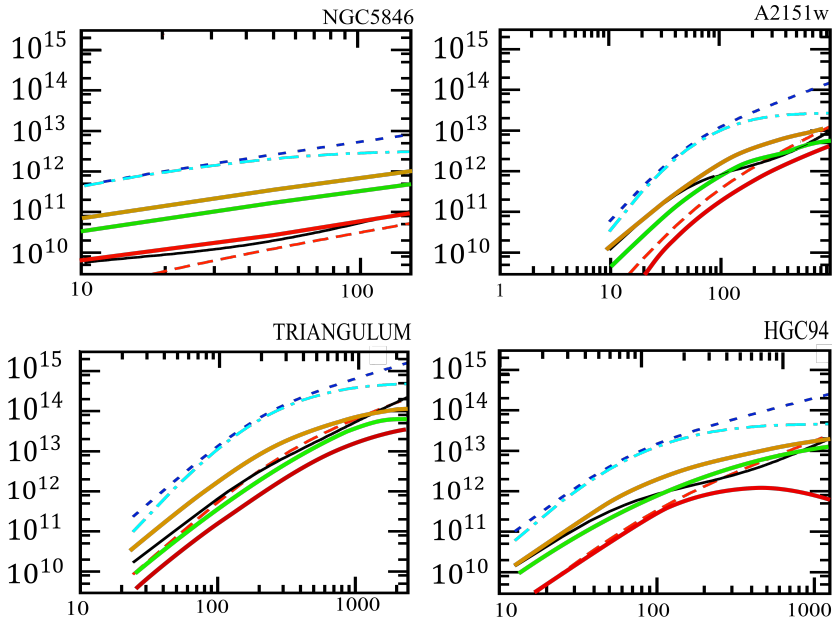

Figure 3 Continued galaxy cluster mass profiles

Table 1 Galaxy cluster properties

Note - This compilation is issued from Brownstein and Moffat (2006). We have added a column for the mass M_κ.

Column (1) Galaxy cluster name

Column (2) X-ray temperature

Column (3) ICM central mass density

Column (4) model parameter

Column (5) model core radius parameter

Column (6) radius where gas $\simeq 10^{-28}$ $g\ cm^{-3}$

Column (7) ICM gas mass integrated to r_{out}

Column (8) Newtonian dynamic mass integrated to rout

Column (9) MSTG dynamic mass integrated to rout

Column (10) convergent MOND dynamic mass

Column (11) M_κ integrated to rout

Cluster	T keV	ρ_M $10^{-25}\ g\ cm^{-3}$	β	r_c kpc	r_{out} kpc	M_{gas} $10^{14} M_\odot$	M_N	M_{MSTG}	M_{MOND}	M_κ
(1)	(2)	(3)	(4)	(5)	(6)	(7)	(8)	(9)	(10)	(11)
A0085	6.90	0.34	0.532	58.5	2,241	1.48	9.02	1.15	1.83	0.77
A0119	5.60	0.03	0.675	352.8	1728	0.73	6.88	0.73	1.76	0.60
A0133	3.80	0.42	0.530	31.7	1417	0.37	3.13	0.28	0.55	0.27
NGC507	1.26	0.23	0.444	13.4	783	0.05	0.48	0.02	0.04	0.04
A0262	2.15	0.16	0.443	29.6	1334	0.26	1.39	0.11	0.13	0.12
A0399	7.00	0.04	0.713	316.9	1791	0.90	9.51	1.07	3.07	0.82
FORNAX	1.20	0.02	0.804	122.5	387	0.009	0.373	0.011	0.102	0.026
NGC1550	1.43	0.15	0.554	31.7	632	0.034	0.548	0.024	0.086	0.047
A1060	3.24	0.09	0.607	66.2	790	0.07	1.69	0.10	0.50	0.21
A1367	3.55	0.03	0.695	269.7	1234	0.27	3.19	0.26	0.75	0.40
MKW4	1.71	0.57	0.440	7.7	948	0.09	0.78	0.05	0.08	0.10
ZwCl1215	5.68	0.05	0.819	303.5	1485	0.59	7.15	0.72	2.5	0.91
NGC4636	0.76	0.33	0.491	4.2	216	0.001	0.088	0.001	0.019	0.011
A3526	3.68	0.29	0.495	26.1	1175	0.20	2.35	0.17	0.45	0.24
A3266	8.00	0.05	0.796	397.2	1,915	1.22	12.82	1.56	4.79	1.12
A3395s	5.00	0.03	0.964	425.4	1223	0.32	5.77	0.49	2.34	0.50
COMA	8.38	0.06	0.654	242.3	1954	1.13	11.57	1.38	3.81	0.99
A2065	5.50	0.04	1.16	485.9	1302	0.49	8.01	0.76	3.83	0.69
A2142	9.70	0.27	0.591	108.5	2537	2.39	15.93	2.32	4.36	1.37
A2244	7.10	0.23	0.607	88.7	1773	0.84	8.36	0.92	2.45	0.71
UGC03957	2.58	0.09	0.740	100.0	764	0.08	1.57	0.09	0.47	0.13
S636	1.18	0.01	0.752	242.3	742	0.06	0.65	0.03	0.09	0.05
M49	0.95	0.26	0.592	7.7	177	0.001	0.109	0.002	0.041	0.009
A1689	9.23	0.33	0.690	114.8	1898	1.23	13.21	1.61	5.14	1.13
A1800	4.02	0.04	0.766	276.1	1284	0.34	4.14	0.36	1.15	0.38

A1914	10.5	0.22	0.751	162.7	1768	1.08	15.21	1.79	7.44	1.31
NGC5813	0.52	0.18	0.766	17.6	166	0.001	0.072	0.001	0.021	0.006
NGC5846	0.82	0.47	0.599	4.9	152	0.001	0.082	0.001	0.031	0.007
A2151w	2.40	0.16	0.564	47.9	957	0.12	1.42	0.09	0.25	0.12
TRIANGULUM	9.60	0.1	0.61	196.5	2385	1.98	15.22	2.11	4.48	1.32
OPHIUCHUS	10.3	0.13	0.747	196.5	1701	0.91	14.11	1.59	6.91	1.21
ZwC174	5.23	0.1	0.717	163.4	1354	0.43	5.49	0.50	1.79	0.47
A3888	8.84	0.1	0.928	282.4	1455	0.71	12.61	1.33	7.14	1.08
HGC94	3.45	0.11	0.514	60.6	1237	0.24	2.40	0.19	0.43	0.21
RXJ2344	4.73	0.07	0.807	212.0	1222	0.34	4.97	0.43	1.78	0.43

By comparing columns 9 and 11 in Table 1, MOG and κ-model provide reasonably close values to each other for the masses integrated to rout, respectively M_{MSTG} and M_κ. By comparing columns 7 and 11 in Table 1, the agreement between M_κ and M_{gas} is fairly good, and it is clear that, in most cases, the κ-model does not necessitate dark matter in the outer regions of the galaxy clusters. In Table 1, M_κ is smaller than M_{MSTG} when the temperatures are higher than $5-6\ keV$, whereas the reverse is true when the temperatures are lower than $5-6\ keV$. On the other hand, for $T\sim 5-6\ keV$, then $M_\kappa \sim M_{MSTG}$. Eventually, when the temperatures are smaller than $1\ keV$, then M_κ are larger than M_{MSTG}.

By contrast, convergent MOND dynamic mass, M_{MOND}, are systematically located too high. Even though MOND substantially decreases the dark matter content for convergent MOND dynamic mass, this theory is not able to completely remove dark matter in the galaxy clusters. By comparing the columns 10 (M_{MOND}) and 7 (M_{gas}) of Table 1, M_{MOND} is sometimes superior by a mean factor of the order of 2 to M_{gas}. Galaxy cluster stability cannot be fully explained by the current MOND formulation alone. MOND, at least its initial

form (Milgrom, 1983), still needs to use a residual content of invisible matter for galaxy clusters. However, owing to the great success of MOND for the individual galaxies, a proper direction is to build a multiscale MOND, which is able to simultaneously explain both individual galaxies and galaxy clusters. Fortunately, this model has been built. This is the main motivation of EMOND; EMOND assumes that there is an increase in the fundamental parameter a_0 of the MOND paradigm in galaxy clusters compared to the value selected for this coefficient in the case of individual galaxies (Zhao and Famaey, 2012; Hodson and Zhao, 2017 a, b). This rescaling adapts the parameter a_0 to the size of the object under consideration and appears to be quite natural. In this case, MOND can eventually and adequately fit the ICM gas mass integrated to r_{out}. Note, in the context of the κ-model a physical interpretation of this rescaling in MOND is supplied. The mean density in a galaxy cluster is much smaller than the corresponding one in an individual galaxy by a factor ~ 40 (center of the cluster) and $\sim 200 - 1000$ (in the outskirts of the cluster). In our study, the rescaling is given by an estimate of κ, and $\kappa_G/\kappa_{cluster} \sim 5 - 10$.

Despite these promising considerations for the κ-model, MOG appears to be slightly better as for the fitting of the observational curves. We might argue that MOG has two free outer parameters, whereas the κ-model has none; therefore, it is easier to fit a curve with a sufficient number of outer free parameters than without any free parameter. However, on closer examination of MOG, we can see that a multifit procedure is used throughout the calculations. MOG relies on two parameters M_0 and r_0, but these parameters are not constant across the series of galaxy clusters. Moreover, M_0 depends on the ICM gas mass for each individual clusters (Brownstein and

Moffat, 2006, paragraph 4). Thus it seems that in MOG the results are already included at the start of the calculations, and the method appears somewhat post hoc. Thus, MOG is not a fully ab initio procedure. Due to these reasons, the κ-model and EMOND are more efficient than MOG as for their predictive power.

4 Bullet Cluster

The Bullet Cluster (1E 0657-56) is very often presented as a clear proof of the existence of dark matter (Figure 3). The Bullet Cluster is composed of two colliding clusters: a main cluster (Mc) and a small or sub-cluster (Sc) (the bullet per se) (Bradač el al, 2005, 2006).

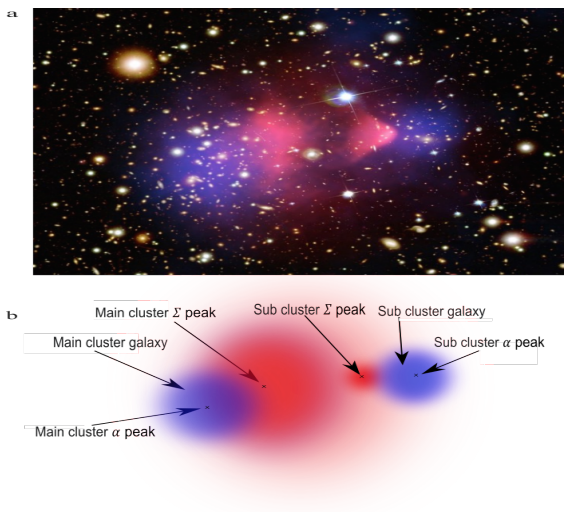

Figure 4

To determine how the κ-model reinterprets the observational data for the Bullet Cluster, we initially start with the known (but apparent) surface densities for both the hot gas and the visible galaxies (Figure 5). Figures 5a and 5b are reproduced from Brownstein and Moffat (2006). In addition, Table 2 provides the masses for the different components. The assumed DM content is adjusted such that the total mass ratio DM/B is ~ 6.

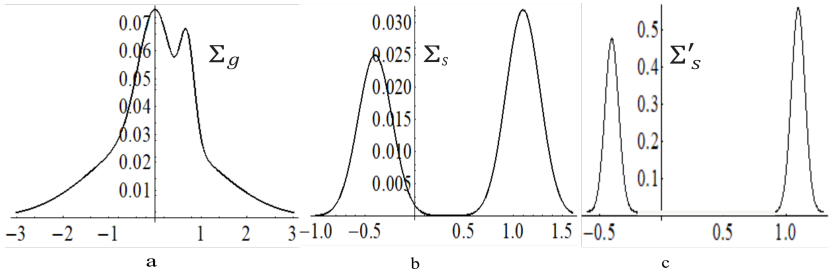

Figure 5

Figure 5 Abscissa : distances, unit 500 kpc. Ordinate: surface densities, unit 3.1 10^3 $M_\odot$ pc^{-2}. The abscissa axis passes through the galaxy cluster centers. Figure 5a: scaled plot of hot gas density, Figure 5b: scaled plot of apparent galaxy density observed from Earth (Main cluster + Bullet) and Figure 5c: scaled plot of real galaxy density measured by a hypothetical observer located inside the Main or the Sub group of visible galaxies (represented by blue disks in Figure 4). The mass is invariable by the transform: apparent $\longleftrightarrow$ real surface densities, i.e. $\int dxdy\ \Sigma_s(x,y) = \int dxdy\ \Sigma'_s(x,y)$.

Component	Main cluster (Main)	Subcluster (Sub)	Diffuse component	Total
M_{gas}	4.38 10^{13}	1.93 10^{13}	8.01 10^{13}	1.43 10^{14}
$M_{galaxies}$	4.67 10^{12}	3.46 10^{12}	–	8.32 10^{12}
M_{DM}	6.54 10^{14}	1.67 10^{14}	–	8.21 10^{14}

Table 2 The masses are expressed in solar mass $M_\odot$

In the usual treatment of the galaxy clusters (paragraph 2), only the gaseous component are considered (the stellar fraction is negligible in galaxy clusters). In the specific case of the Bullet Cluster, the situation is very different. We have two clearly identified parts: a very massive gaseous component and a galactic component; however, these two components are separated. Based on the lensing diagram, only the gaseous component needs to be considered in the calculation of κ. Thus, if we assume that the Main and Sub groups of visible

galaxies (the disks displayed in blue in Figure 6) have a low content of gas, the lensing due to the κ effect is much higher than that in the hot gas (the disk displayed in red in Figure 6). The usual relationship of the κ-model is as follows:

$$\frac{\kappa_M}{\kappa} = 1 + Ln\ \left(\frac{\Sigma_M}{\Sigma_{gas}}\right) \tag{20}$$

where $\Sigma_M \sim 0.075 \times 3.1\ 10^3\ M_\odot\ pc^{-2} = 232.5\ M_\odot\ pc^{-2}$ is the maximal value taken by the surface density of hot gas (Figure 5a). Figure 5a can be used to provide the following relationship:

$$\left(\Sigma_{gas}^{Main}\right)_{outer}\ ,\ \left(\Sigma_{gas}^{Sub}\right)_{outer}\ \sim 0.7 \times 232.5\ M_\odot\ pc^{-2} = 162.7\ M_\odot\ pc^{-2} \tag{21}$$

The latter quantity represents the surface density of the hot gas located in the immediate environment of the Main and Sub groups of visible galaxies; each of them being displayed by a blue disk in Figure 4.

However, following the current interpretation, both the Main and Sub galaxy clusters were stripped from the hot gas during the collision. The amount of the gas remaining inside the groups of visible galaxies after this collision needs to be determined. Clearly the hot gas initially located inside the Main and Sub groups of visible galaxies is removed by the strong shock during the collision, and each of these groups is now located in a subdense bubble with a low content of hot gas. A pre-analysis of the α-diagram in the κ-model context, compared to that provided by observations (Bradač el al, 2005, 2006), enables to predict that the amount of hot gas inside the subdense bubbles is $\sim$ 15% of the amount of hot gas surrounding them, i.e. $\left(\Sigma_{gas}^{Main}\right)_{inner}$ or $\left(\Sigma_{gas}^{Sub}\right)_{inner} = 24.4\ M_\odot\ pc^{-2}$. With equal

temperatures, the gas pressure in the groups of visible galaxies (blue regions in the Figure 4) is thus predicted to be lower than that in the immediate region surrounding them (red region). Evidently, the system is not in hydrostatic equilibrium, and this situation cannot indefinitely persist. The required time to re-equalize the densities is approximately $\frac{R_c}{3c_s} \sim 100\ Myears$, where $R_c \sim 0.5\ Mpc$ is the mean characteristic size of the Main or Sub groups of visible galaxies and c_s is the speed of sound in the hot gas ($T_e \sim 10^8\ K$)[9]. With the relationship (10) and the aforementioned values of $(\Sigma_{gas}^{Main})_{inner}$ or $(\Sigma_{gas}^{Sub})_{inner}$, we can determine the amplification factor κ inside the two groups of visible galaxies as follows:

$$\frac{\kappa_M}{\kappa_{gas}^{Main}} = \frac{\kappa_M}{\kappa_{gas}^{Sub}} \sim \frac{\kappa_M}{\kappa_{gas}^{galactic}} = 3 \tag{22}$$

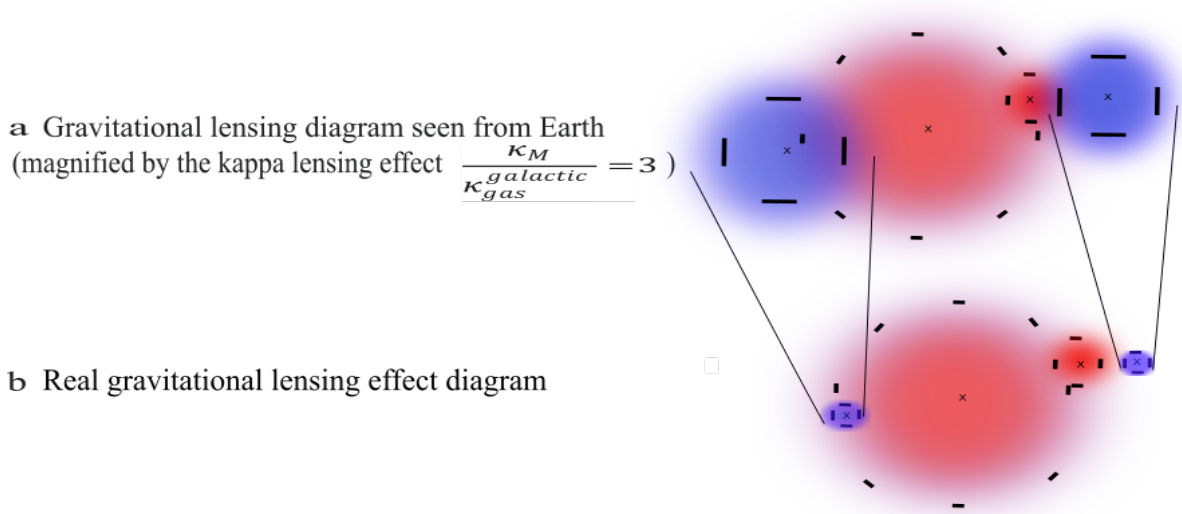

Figure 6 Basic illustration of the combined action of both gravitational and kappa lensings. The lensing by the hot gas is used as a reference for the two figures a and b.

[9]After this short period of time, the κ-model predicts that the lensing diagram will no longer be centered on the groups of visible galaxies, but on the hot gas and will likely resemble Figure 7a. Thus, we see an instantaneous phase of a rapidly evolutionary process.

In Figure 6a, the combined product of both the gravitational and kappa lensing effects is clearly centered on the Main and Sub groups of visible galaxies. In Figure 6b, as expected, the lensing is clearly centered on the hot gas (which contains 90% of the baryonic mass against 10% for the visible galaxies in a galaxy cluster). However, the reality shown in Figure 6b cannot be viewed by a unique observer (for instance, a terrestrial observer surrounded by its own environment). Specifically, two distinct observers are needed to determine the effect. The part located in the blue area (groups of visible galaxies) is perceived by a hypothetical observer situated inside any region where the mean gas density is the same as that in the Main or Sub group of visible galaxies; the part located in the red area (hot gas) is perceived by a hypothetical observer situated inside any region where the mean density is the same as that in the hot gas. If the κ-model paradigm is expected to be on the right track, then the Bullet Cluster is an illustrative (but rare) example that the perception of the objects in the Universe is observer-dependent.

Beyond these qualitative considerations, calculations are evidently needed to ascertain our purpose. The procedure is well known. The field equations of general relativity can be linearized if the gravitational field is weak. Then, the deflection angle of a set of masses is simply the vectorial sum of the deflections due to individual lenses. The plane of the sky is $(x,\ y)$. The deviation angle $\boldsymbol{\alpha}$ can be written using the thin lens approximation as follows(Bartelmann and Schneider, 2001):

$$\boldsymbol{\alpha}\left(x,y\right)=\int_{S}dx'dy'\frac{4G}{c}\Sigma(x',y')\frac{\mathbf{r}-\mathbf{r}'}{\left|\mathbf{r}-\mathbf{r}'\right|^{2}} \tag{23}$$

where G is the gravitational constant and c is the speed of light. The density distribution Σ is integrated over all the surface S of the

cluster system. The total surface density $\Sigma(x,y)$ is the sum of the gas and stellar surface densities.

$$\Sigma(x,y) = \Sigma_g(x,y) + \Sigma'_s(x,y) \tag{24}$$

where $\Sigma_g(x,y)$ and $\Sigma'_s(x,y)$ are the fits of the distributions represented in Figures 4a and 4c, respectively; these are assumed to be approximately circular and Gaussian.
We know that the κ-model does not change the local physics, apart from a magnification factor locally applied. Thus, in the κ-model, the relationship (14) eventually becomes the following:[10]

$$\boldsymbol{\alpha}(x,y) = \int_S dx'dy' \frac{4G}{c} \left[\Sigma_g(x,y) + \frac{\kappa_M}{\kappa_{gas}^{galactic}} \Sigma'_s(x,y) \right] \frac{\mathbf{r}-\mathbf{r}'}{|\mathbf{r}-\mathbf{r}'|^2} \tag{25}$$

Figure 7 shows the lensing diagrams $|\boldsymbol{\alpha}|$ of both dark matter and κ-model and Figure 8 shows the components α_x and α_y. Even though the physical interpretation is very different, the κ-model and DM diagrams are very similar and both show that the lensing is centered on the visible galaxies and not on the hot gas, which is centered at $(0,0)$. The essential difference between the two models is that the κ-model does not need dark matter to explain the same facts.

[10] A multiplicative factor, $\frac{\kappa_E}{\kappa_M}$, needs to be applied to $\alpha(x,y)$; however, the factor is a global and constant coefficient independent of x, y, which does not affect the relative position of the peaks on the lensing diagram.

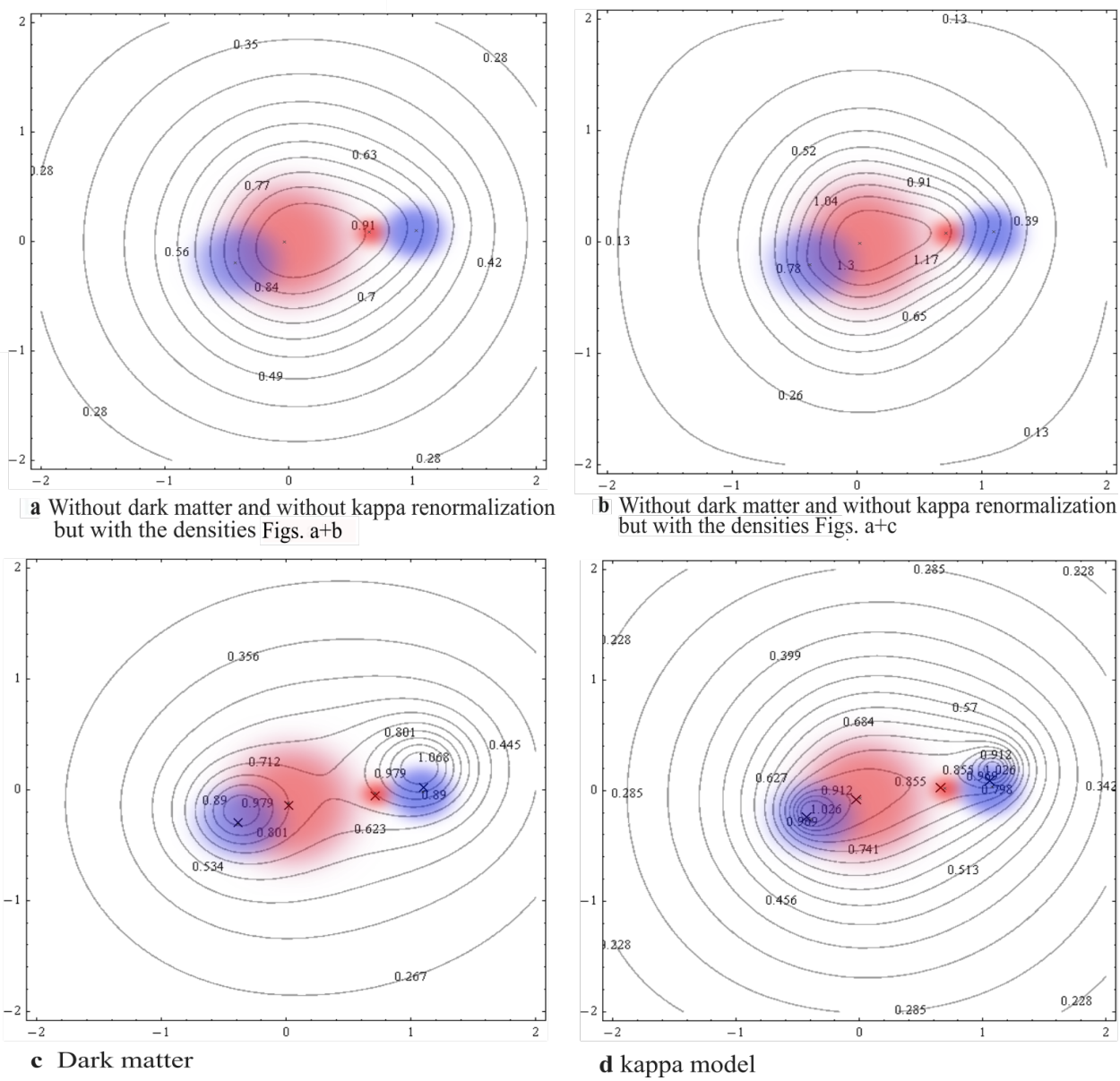

a Without dark matter and without kappa renormalization but with the densities Figs. a+b

b Without dark matter and without kappa renormalization but with the densities Figs. a+c

c Dark matter

d kappa model

Figure 7 Comparative plots of the lensing diagram. The crosses indicate the positions of the centers of the different distributions (hot gas in red and groups of visible galaxies in blue)

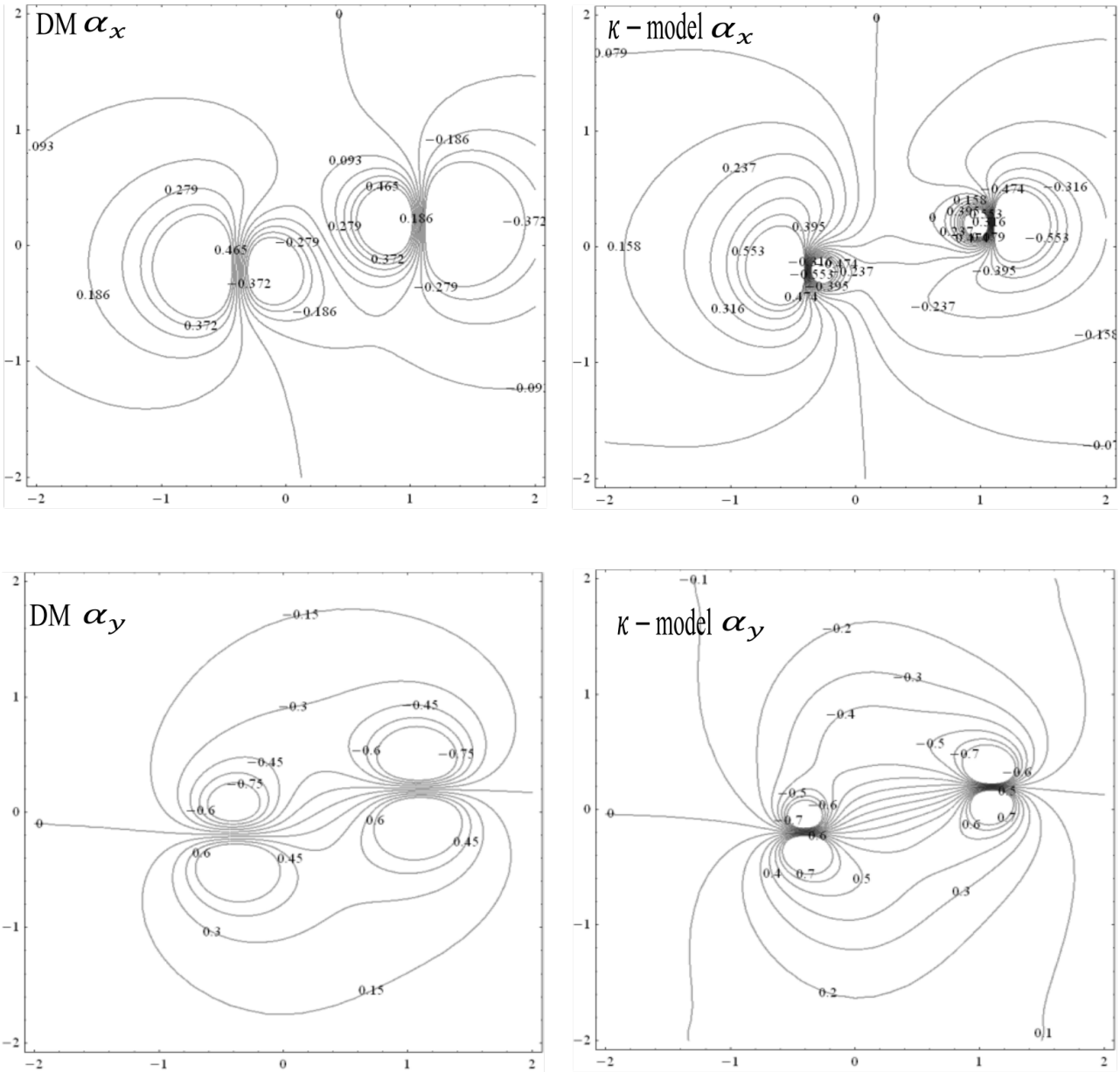

Figure 8 The same as Figure 7 but for the components of $\boldsymbol{\alpha}$

The method applied to the Bullet Cluster can be extended to other similar cases such as the Train Wreck Cluster (Abell 620). In the latter situation the lensing is centered on the hot gas. Even though the morphology of the Train Wreck Cluster is much more complex than that of the Bullet Cluster (Jee et al, 2014), a natural explanation in the framework of the κ-model is that the intergalactic gas filling rate of the bubbles containing the visible galaxies is different. With

a filling rate of 60% instead of 15% (Bullet Cluster) we have been able to ascertain that the lensing is no longer centered on the visible galaxies.

5 Conclusion

Effectively tested MOND and MOG models were designed to understand the dynamics of the Universe without dark matter. By contrast, the dark matter paradigm is an ad hoc concept, where the dark matter content has to be adapted to each situation and consequently, has no predictive value. However, and paradoxically enough, the DM paradigm constitutes a near unanimous recognition among the astrophysicists. The main reason is that the DM paradigm is very easy to use and effectively works at all times due to its extreme flexibility.

On the other hand, in the framework of the κ-model, the single issue of the baryonic mass needs to be sufficient to understand the dynamics of galaxies and that of the galaxy clusters, without dark matter or artificial ingredients, such as the introduction of new parameters into the calculations. Specifically, the κ-model aims to determine a one-to-one relationship directly linking the sole observational data, i.e. the estimated mean density, to either the spectroscopic velocities in the galaxies or X-ray temperatures in galaxy clusters. The κ-model is a MOND-type model, and a behavior very similar to MOND needs to be found for the galaxy clusters. In reality, even though the shape of curves are effectively similar, the κ-model curves are strongly parallel-displaced and systematically move closer to the observational curves than MOND. The agreement between the κ-model prediction and the observational data for the total mass of the hot gas in a galaxy cluster is satisfactory when the mass ratio

DM/B is less than 10, but for values exceeding this ratio the observational total mass of gas cannot be effectively predicted in the framework of an isothermal model. In this case, a lower temperature for the hot gas is predicted in the inner regions of the galaxy clusters.

Finally, the ordered series is as follows: the κ-model has no outer parameter (except the internal parameters relative to the system type (individual galaxies or galaxy clusters), i.e. mean density and temperature); MOND is similar with just a single outer parameter; MOG has two outer parameters (unfortunately, it is in fact a disguised gas-mass dependent multifit parameter for the galaxy clusters, i.e. the results are already included in the hypotheses), and DM is an artificial and ad hoc procedure that works at all times. Our proposed logical program was developed to fit the observational curves with only the observational parameters in a self-consistent manner (i.e. through the triplet mean densities, spectroscopic velocities, and temperatures), and this ultimate goal is now possible in the framework of the κ-model.

Acknowledgment : the author wishes to thank the anonymous reviewers for useful comments and suggestions.

Data availability statement: The author confirms that the data supporting the findings of this study are available within the article and the reference list.

Conflicts of Interest: The author declares no conflict of interest.

6 References

Banik, I. & Zhao, H., 2022, Symmetry, 14, 1331
Bartelmann, M., & Schneider, P., 2001, Physics Reports, 340, 291

Bradač, M., Schneider, P., Lombardi, M., & Erben, T., 2005, A & A, 436, 39
Bradač, M., Clowe, D., Gonzalez, A.H., Marshall, P., Forman, W., Jones, C., Markevitch, M., 2006, ApJ, 652, 937
Randall, S., Schrabback, T., & Zaritsky, D., 2006, ApJ, 652, 937
Browstein, J.R., & Moffat, J., 2006, MNRAS, 367, 527
Browstein, J.R., & Moffat, J., 2007, MNRAS, 382, 29
Bykov, A.M., Churazov, E.M., Ferrari, C., Forman, W.R. Kaastra, J.S., Klein, U., Markevitch, M., & J. de Plaa, J., 2015, Space Sci Rev, 188:141
Calcagni, G., Adv. Theor. Math. Phys., 2012, 16, 549
Capozziello, S., & De Laurentis, M., 2012, Ann. D. Physik, 524, 545
Cavaliere, A. L. & Fusco-Femiano, R. 1976, A&A, 49, 137
DAMA/LIBRA Collaboration, 2022, arXiv.2208.05158
Famaey, B, & McGaugh, S., 2012, Living Rev. Relativity 15, 10
Freundlich, J., Famaey, B., Oria, P.A., Bílek, M., Müller O, & Ibata, R., 2022, A&A, 658, A24
Giunti, C, & Lasserre, T., 2019, Annual Review of Nuclear and Particle Science, Volume 69, 163
Hodson, A.O,. & Zhao H., 2017a, A&A, 598, A127
Hodson, A.O,. & Zhao H., 2017b, A&A, 608, A109
Jee, M. J., Hoekstra, H., Mahdavi, A., & Babul, A., 2014, ApJ. 783 (2): 78
Mc Gaugh, S., 2015, Canadian Journal of Physics. 93 (2): 250
McGaugh, S.S., Lelli, F., & Schombert, J. M. 2016, Physical Review Letters, 117, 201101
Mannheim, P.D., & Kazanas, D., 1989, ApJ, 342, 635
Milgrom, M. 1983, Astrophys. J. 270, 365
Milgrom, M., Canadian Journal of Physics, 2015, 93(2): 107

Moffat, J. W.,2006, Journal of Cosmology and Astroparticle Physics, 3, 4
Moffat, J.W., 2020, Eur. Phys. J. C, 80(10), 906
Niikura, H., Takada, M., Yasuda, N., Lupton, R.H., Sumi, T., More, S., Kurita, T., Sugiyama, S., More, A., Oguri, M., & Chiba, M., 2019, Nature Astronomy, 3, 524
O'Brien, J.G., & Moss, R.J., 2015, J. Phys.: Conf. Ser. 615, 012002
Pascoli, G. & Pernas, L., 2020, hal: 02530737
Pascoli, G, 2022a, Astrophys. and Space Sci., 367, 121
Pascoli, G., 2022b, arXiv: 2205.03062
Reiprich, T.H, 2001, Ph.D.Dissertation, Cosmological Implications and Physical Properties of an X-Ray Flux-Limited Sample of Galaxy Clusters, Ludwig-Maximilians-Universität München
Reiprich, T.H. & Böhringer, H. 2002, ApJ, 567, 716
Schödel,R. Gallego-Cano, E., Dong, Nogueras-Lara, F., Gallego-Calvente, A.T., Amaro-Seoane, P. & Baumgardt, H., 2018, A&A, 609, A27
Skordis, C, & Złośnik, T., 2021, Phys. Rev. Lett., 127, 161302
Varieschi, G.U., 2020, Found Phys 50, 1608
Varieschi, G.U. & Calcagni, G., 2022, JHEP, 2022, 24
Varieschi, G.U., 2023, Universe, 9, 246
Verlinde, E.P., 2017, SciPost Phys. 2, 016
Walker, S., Simionescu, A., Nagai D., Okabe, N., Eckert, D., Mroczkowski, T., Akamatsu, H., Ettori, S., & Ghirardini, V., 2019, Space Science Reviews, 215: 7
Watanabe, M., Yamashita, K., Furuzawa, A., Kunieda, H., & Tawara, Y., 1999, ApJ, 527: 80
Xenon Collaboration, 2023, arxiv2303.14729v1
Zhao, H., & Famaey, B., 2012, Phys. Rev. D, 86, 067301

Appendix A : Case of an extended set of points

As discussed in section 2, in the κ-model, the dynamic equation, formally written for an infinitesimal element of matter of mass dm and subjected to a force $d\boldsymbol{f}$, is as follows:

$$dm\frac{d}{dt}\left(\kappa\dot{\boldsymbol{\sigma}}\right) = d\boldsymbol{f} \tag{26}$$

where κ is a local normalization coefficient applied to the spatial lengths and $d\boldsymbol{f}$ is measured in situ, i.e. where the element of matter resides. However, this equation has no meaning without a reference frame predefined in advance. First, the internal motions of any particle (a star, a nebula) in a galaxy needs to be studied in the reference frame R_A, in which the barycenter of the galaxy is at rest. Such a reference frame can be built by considering a collection $S_{\{A_i\}}$ of open sets U_{A_i} which entirely covers the galaxy. A couple $(A_i,\ \kappa_{A_i})$, composed of an observer A_i and a normalization coefficient applied to the spatial lengths, κ_{A_i}, is associated with each open set U_{A_i}. The observers A_i are assumed to be at rest relatively to each other, as follows:

$$\boldsymbol{v}(A_i)_{A_j} = \boldsymbol{0} \tag{27}$$

Then, the collection $S_{\{A_i\}}$ composes a reference frame R_A. The observers A_i do not use the same unit of length along R_A, but they are at rest relatively to each other as imposed by eq. (28). Next, for any point P in the set U_{A_i}, the following relationship is used:

$$\boldsymbol{v}(P)_{A_i} = \kappa_{A_i}\dot{\boldsymbol{\sigma}}(P)_{A_i} \tag{28}$$

Second, the motion of any galaxy as a whole has to be treated as if this one was a point confounded with its barycenter. Any galaxy

evolves in a cluster of galaxies. A second collection $S_{\{B_l\}}$ of open sets U_{B_l} is considered and once again covers the entire galaxy cluster. The observers B_l are assumed to be at rest relatively to each other, as follows:

$$\boldsymbol{v}(B_l)_{B_m} = \mathbf{0} \tag{29}$$

Then, the collection S_{B_l} constitutes a second reference frame R_B. A couple (B_l, κ_{B_l}), composed of an observer B_l and a normalization coefficient applied to the spatial lengths, κ_{B_l}, is associated to each open set U_{B_l}. For any couple of sets U_{A_i} and U_{A_j} located in a set U_{B_l}, we have the following relationships:

$$\dot{\boldsymbol{\sigma}}(A_i)_{B_l} = \dot{\boldsymbol{\sigma}}(A_j)_{B_l} \tag{30}$$

and

$$\boldsymbol{v}(A_i)_{B_l} = \kappa_{B_l} \dot{\boldsymbol{\sigma}}(A_i)_{B_l} \tag{31}$$

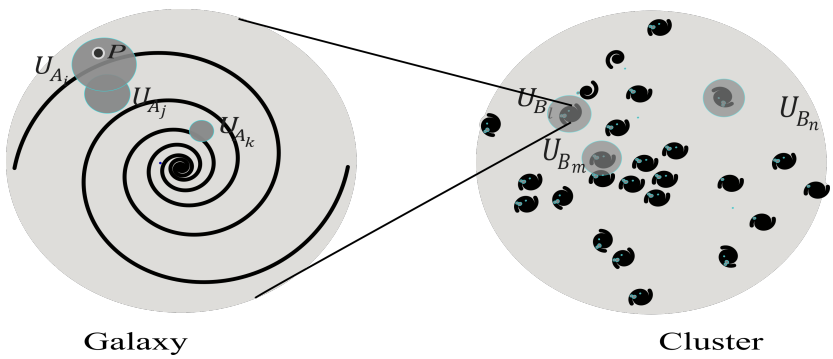

Figure 9

The law of addition of velocities is applied, as follows:

$$\boldsymbol{v}(P)_{B_l} = \boldsymbol{v}(P)_{A_i} + \boldsymbol{v}(A_i)_{B_l} \tag{32}$$

with the following: $\boldsymbol{v}(P)_{A_i} = \kappa_{A_i} \dot{\boldsymbol{\sigma}}(P)_{A_i}$, $\boldsymbol{v}(A_i)_{B_l} = \kappa_{B_l} \dot{\boldsymbol{\sigma}}(A_i)_{B_l}$.

Based on these relationships, the expression (25) can now be properly rewritten ($d\boldsymbol{f}_i$ represents the internal forces, $d\boldsymbol{f}_{inertial}$, $d\boldsymbol{f}_e$ are the inertial forces and the external forces, respectively, applied on the mass dm), as follows:

$$dm\frac{d}{dt}(\kappa_{A_i}\dot{\boldsymbol{\sigma}}\left(P\right)_{A_i}) = d\boldsymbol{f}_i + d\boldsymbol{f}_{inertial} + d\boldsymbol{f}_e \tag{33}$$

This equation treats the case of the internal motions within the galaxy (for instance, the rotation). We can integrate eq. 34 over the volume Ω of the galaxy, as follows:

$$\int_\Omega dm\frac{d}{dt}(\kappa_{A_i}\dot{\boldsymbol{\sigma}}\left(P\right)_{A_i}) = \int_\Omega d\boldsymbol{f}_i + \int_\Omega d\boldsymbol{f}_{inertial} + \int_\Omega d\boldsymbol{f}_e = \boldsymbol{F}_i + \boldsymbol{F}_{inertial} + \boldsymbol{F}_e \tag{34}$$

For an isolated ($\boldsymbol{F}_e = \boldsymbol{0}$, $\boldsymbol{F}_{inertial} = \boldsymbol{0}$) and symmetric ($\boldsymbol{F}_{i\ asym} = 0$) galaxy, the following relationship is obtained:

$$\int_\Omega dm\ \kappa_{A_i}\dot{\boldsymbol{\sigma}}\left(P\right)_{A_i} = \boldsymbol{K} \tag{35}$$

where the constant $\boldsymbol{K}$ can eventually considered nul.

The dynamic equation for a symmetric galaxy studied as a whole and covered by a set B_l is as follows: [11]

$$M\frac{d}{dt}(\kappa_{B_l}\dot{\boldsymbol{\sigma}}(A_i)_{B_l}) = \boldsymbol{F}_e \tag{37}$$

where M is the total mass of the galaxy ($M = \int_\Omega dm$)). The equation (38) can be used to treat the motion of a galaxy (viewed as

[11] For an isolated and asymmetric galaxy for which $\boldsymbol{F}_{i\ asym} \neq \boldsymbol{0}$, this equation becomes the following:

$$M\frac{d}{dt}(\kappa_{B_l}\dot{\boldsymbol{\sigma}}(A_i)_{B_l}) = \boldsymbol{F}_{i\ asym} \tag{36}$$

In this case, the galaxy can be auto-accelerated.

a point here) in a galaxy cluster. The dynamic equation (34) relative to any point P of mass m in the galaxy becomes:[12]

$$m(\frac{d}{dt}\kappa_{A_i}\dot{\boldsymbol{\sigma}}\left(P\right)_{A_i}) = \boldsymbol{f}_i + (\boldsymbol{f}_e - \frac{m}{M}\boldsymbol{F}_e) \tag{39}$$

The force $\boldsymbol{f}_e - \frac{m}{M}\boldsymbol{F}_e$ is the tidal force produced by an outer mass. Equation (40) can be used to treat the internal motions in a galaxy.

[12]Let P contained in the set A_i and P' contained in the set $A_{i'}$ The internal forces are calculated as follows:

$$\boldsymbol{f}_{P'\longrightarrow P} = -G\frac{\kappa_{A_i}}{\kappa^3_{A_i}}\frac{\boldsymbol{P'P}}{P'P^3} \qquad \boldsymbol{f}_{P\longrightarrow P'} = -G\frac{\kappa_{A_{i'}}}{\kappa^3_{A_{i'}}}\frac{\boldsymbol{PP'}}{PP'^3} \tag{38}$$

The force needs to be measured in situ (i.e. respectively at P for $\boldsymbol{f}_{P'\longrightarrow P}$ and at P' for $\boldsymbol{f}_{P\longrightarrow P'}$) and, in this case, the measured force is a well-defined quantity and considered observer-independent.